Nanotoxicology

ISSN: 1743-5390 (Print) 1743-5404 (Online) Journal homepage: https://www.tandfonline.com/loi/inan20

# Low-dose exposure of silica nanoparticles induces cardiac dysfunction via neutrophil-mediated inflammation and cardiac contraction in zebrafish embryos

Junchao Duan, Yang Yu, Yang Li, Yanbo Li, Hongcui Liu, Li Jing, Man Yang, Ji Wang, Chunqi Li & Zhiwei Sun

**To cite this article:** Junchao Duan, Yang Yu, Yang Li, Yanbo Li, Hongcui Liu, Li Jing, Man Yang, Ji Wang, Chunqi Li & Zhiwei Sun (2016) Low-dose exposure of silica nanoparticles induces cardiac dysfunction via neutrophil-mediated inflammation and cardiac contraction in zebrafish embryos, Nanotoxicology, 10:5, 575-585, DOI: 10.3109/17435390.2015.1102981

**To link to this article:** https://doi.org/10.3109/17435390.2015.1102981

http://informahealthcare.com/nan
ISSN: 1743-5390 (print), 1743-5404 (electronic)

Nanotoxicology

Nanotoxicology, 2015; 10(5): 575–585
 DOI: 10.3109/17435390.2015.1102981

Taylor & Francis
Taylor & Francis Group

ORIGINAL ARTICLE

# Low-dose exposure of silica nanoparticles induces cardiac dysfunction via neutrophil-mediated inflammation and cardiac contraction in zebrafish embryos

Junchao Duan[1,2], Yang Yu[1,2], Yang Li[1,2], Yanbo Li[1,2], Hongcui Liu[3], Li Jing[1,2], Man Yang[1,2], Ji Wang[1,2], Chunqi Li[3], and Zhiwei Sun[1,2]

[1]*School of Public Health, Capital Medical University, Beijing, P.R. China,* [2]*Beijing Key Laboratory of Environmental Toxicology, Capital Medical University, Beijing, P.R. China, and* [3]*Hunter Biotechnology Inc., Hangzhou, Zhejiang Province, P.R. China*

**Abstract**

The toxicity mechanism of nanoparticles on vertebrate cardiovascular system is still unclear, especially on the low-level exposure. This study was to explore the toxic effect and mechanisms of low-dose exposure of silica nanoparticles (SiNPs) on cardiac function in zebrafish embryos via the intravenous microinjection. The dosage of SiNPs was based on the no observed adverse effect level (NOAEL) of malformation assessment in zebrafish embryos. The mainly cardiac toxicity phenotypes induced by SiNPs were pericardial edema and bradycardia but had no effect on atrioventricular block. Using *o*-Dianisidine for erythrocyte staining, the cardiac output of zebrafish embryos was decreased in a dose-dependent manner. Microarray analysis and bioinformatics analysis were performed to screen the differential expression genes and possible pathway involved in cardiac function. SiNPs induced whole-embryo oxidative stress and neutrophil-mediated cardiac inflammation in Tg(mpo:GFP) zebrafish. Inflammatory cells were observed in atrium of SiNPs-treated zebrafish heart by histopathological examination. In addition, the expression of TNNT2 protein, a cardiac contraction marker in heart tissue had been down-regulated compared to control group using immunohistochemistry. Confirmed by qRT-PCR and western blot assays, results showed that SiNPs inhibited the calcium signaling pathway and cardiac muscle contraction via the down-regulated of related genes, such as ATPase-related genes (*atp2a1l*, *atp1b2b*, *atp1a3b*), calcium channel-related genes (*cacna1ab*, *cacna1da*) and the regulatory gene *tnnc1a* for cardiac troponin C. Moreover, the protein level of TNNT2 was decreased in a dose-dependent manner. For the first time, our results demonstrated that SiNPs induced cardiac dysfunction via the neutrophil-mediated cardiac inflammation and cardiac contraction in zebrafish embryos.

**Keywords**

Cardiac dysfunction, cardiac muscle contraction, inflammation, silica nanoparticles, zebrafish

**History**

Received 17 May 2015
Revised 3 September 2015
Accepted 27 September 2015
Published online 26 October 2015

## Introduction

The 2014 World Health Statistics from World Health Organization (WHO) estimated that the top three causes of the years of life lost (YLL) were ischemic heart disease, lower respiratory infections and stroke (WHO, 2014). It is well documented that the likelihood of cardiovascular diseases and particulate air pollution. A series of scientific statements from the American Heart Association (AHA) point that exposure to elevated levels of particulate matters are strongly linked with heart diseases (Brook et al., 2010; Gold & Mittleman, 2013; Pope et al., 2004). More than 99% of the total number concentration of particles is smaller than 300 nm, and 76% of the particles are in the range of nano-scale (Kumar & Robins, 2010). However, the mechanisms between heart diseases and nano-scale particles (size less than 100 nm) are still debated controversially and its related research conclusions are lack of consistency. Therefore, studying on the cardiovascular toxicity caused by nano-scale particles is very necessary and has a profound scientific significance.

Correspondence: Zhiwei Sun, School of Public Health, Capital Medical University, Beijing 100069, P.R. China. Tel: +86 010 83911507. Fax: +86 010 83911507. E-mail: zwsun@hotmail.com

Silica nanoparticles (SiNPs) are on the priority lists for toxicity evaluation by Organisation for Economic Co-operation and Development (OECD, 2010). SiNPs are one of the most widely used nanomaterials in nano-based products (Hansen et al., 2008). It has multiple exposure pathways, such as environmental exposure, occupational exposure, and iatrogenic exposure (Duan et al., 2014a). Recently, SiNPs are designed as gene therapy or drug delivery carriers in biomedical fields through intravenous injection. The cancer-targeted diagnostic probes, ''C-dots'' that approved by Food and Drug Administration (FDA), are composed by SiNPs and performed for the human clinical trials, Stage I (Benezra et al., 2011). Thus, it raised concerns about the toxicity of SiNPs on cardiovascular system and human health. Although several studies including our previous research had already evaluated the cytotoxicity (Bauer et al., 2011; Duan et al., 2014b; Liu & Sun, 2010), acute toxicity (Yu et al., 2013), and sub-chronic toxicity (Du et al., 2013) of SiNPs in endothelial cells or in mammalian models, information about the toxic effect and its mechanisms of SiNPs on cardiac function is still limited.

Zebrafish are emerging as a promising model for evaluating the early cardiac development and human cardiac disease (Bakkers, 2011; Liu & Stainier, 2012). Cardiomyopathy, disorders

the cardiac muscle, is one of the most common causes for the die of cardiovascular disease in the world (Sogah et al., 2010). It was well known that the cardiac troponin complex, consists of three subunits (troponin C, troponin I, troponin T), is required for normal cardiomyocytes contraction and often used as a target for cardiotonic drugs in the treatment of heart failure (Katrukha, 2013). Mutations of the genes (*tnnc1*, *tnnt2*, *tnni3*) that encode the cardiac troponin complex are associated with a severity of cardiomyopathies (Ferrante et al., 2011). The cardiac development and mature-related genes in zebrafish were similar to human genes. Sogah et al. (2010) found that *tnnc1a* is crucial for the function integrity of cardiomyocytes contractility in zebrafish. Becker et al. (2011) reported that *tnnt2* mutations of zebrafish could lead to severe hypertrophic cardiomyopathy by influenced the handling of calcium in cardiomyocytes.

Previously, we had reported that pericardial edema was the leading causes of SiNPs-induced embryonic malformation in zebrafish, and we also found the cell death of pericardia was increasing significantly, suggested heart might be the target tissue for SiNPs exposure (Duan et al., 2013b). The pericardial edema of zebrafish was also observed in the exposure of titanium dioxide nanoparticles and sliver nanoparticles (Lee et al., 2012; Xu et al., 2012), indicated that it might be a common phenomenon in the cardiac toxicity of zebrafish exposure to nanoparticles. However, the underlying cardiotoxicity mechanism of nanoparticles on zebrafish is still unknown. The recent assessment on the global life cycle releases of nanomaterials showed that a significant fraction of nanomaterials going to soils, water, and atmosphere (Keller et al., 2013). Since the nanoparticles in the ecological environment may affect human health day-by-day, it is meaningful to evaluate the underlying mechanisms of nanoparticles-induced cardiac toxicity at low-dose level, and it will in turn help to understand the cardiovascular toxicity triggered by nano particles *in vivo*.

Using an intravenous microinjection (Duct of Cuvier) method of zebrafish embryos (Benard et al., 2012), this study was conducted to investigate the biological mechanism of SiNPs on heart tissue via blood circulation. The dosage was determined based on the no observed adverse effect level (NOAEL) to evaluate the possible molecular events induced by SiNPs without obvious malformation in zebrafish. The transparent mutant strain (without pigment), Albino zebrafish (Tsetskhladze et al., 2012), was applied to assess the morphological change, heart rate, atrioventricular block, and cardiac output. Microarray analysis and bioinformatics analysis were then performed to screen the differential expression genes and possible pathway related to cardiac function. For in-depth mechanism study, the whole-embryo oxidative stress and inflammation triggered by SiNPs were detected by the neutrophils-tracking transgenic zebrafish strain, Tg(mpo:GFP) (Mathias et al., 2009). Histopathological examination and immunohistochemistry analysis were performed. The differential expression genes in calcium signaling pathway and cardiac muscle contraction were verified, and the cardiac contraction marker protein troponin T (TNNT2) was also determined to clarify whether cardiac muscle contraction was contributed to cardiac dysfunction induced by SiNPs.

## Materials and methods

### SiNPs preparation and characterization

SiNPs were prepared using the Stöber method and characterized as described in our previous studies (Duan et al., 2013b, 2014a,b). Briefly, 2.5 mL of tetraethylorthosilicate (TEOS, Sigma, St. Louis, MO) was added to 50 mL premixed ethanol solution, containing with 2 mL ammonia and 1 mL water. The reaction mixture was kept stirring (150 r/min) at 40 °C for 12 h. After that, the resulting mixture was centrifuged (12 000 r/min, 15 min) to isolate particles. Washing with deionized water three times, the SiNPs were dispersed in ultrapure water (50 mL) as stock medium. Suspensions of SiNPs were dispersed by sonicator (Bioruptor UDC-200, Belgium) for 5 min prior to experimental tests. The size and shape of SiNPs was observed under a transmission electron microscope (TEM, JEOL JEM2100, Akishima-shi, Japan). The hydrodynamic sizes and zeta potential of SiNPs in ultrapure water were detected by Zetasizer (Nano-ZS90, Malvern, Worcestershire, UK). The purity of SiNPs was tested by Inductively Coupled Plasma–Atomic Emission Spetrometer (ICP-AES, ARL 3520, Washington, DC). Using limulus amebocyte lysate (LAL) assay, the endotoxin of SiNPs was determined.

### Zebrafish husbandry

Albino strain zebrafish and Tg(mpo:GFP) strain zebrafish were provided by Hunter Biotechnology, Inc., which is accredited by the International Association for Assessment and Accreditation of Laboratory Animal Care (AAALAC). The accreditation number is 001458. The zebrafish were housed on a circulating aquarium system in an environmentally controlled room (28 °C, 80% humidity). The photoperiod was adjusted to a 14 h light/10 h dark cycle. The larval and adult zebrafish were fed with brine shrimp (hatched from eggs in 10 mL in 2 L salt water) twice a day. The developing embryos and larvae were maintained at 28 °C in fish-husbandry water with 200 mg Instant Ocean Salt (Red Sea, Israel) in 1 L deionized water, conductivity at 4 8 0 ~510 μS/cm, pH for 6.9 ~7.2, and 53.7 ~71.6 mg/L for $CaCO_3$. For experiments, fertilized eggs were collected and chosen under a stereomicroscope (Nikon, SMZ645, Tokyo, Japan) at 6 and 24 hpf (hour post-fertilization). All embryos were derived from the same spawns of eggs for statistical comparison between control and treated groups.

### Intravenous microinjection

Zebrafish embryos were anesthetized with 0.03% tricaine (Sigma, St. Louis, MO) at 48 hpf. The different concentrations of SiNPs was loaded into borosilicate pulled glass capillary needles with an internal diameter of 15 μm and the outer diameter of 18 μm (World Precision Instruments, Sarasota, FL) by an electrode puller (NARISHIGE, PC-10, Tokyo, Japan). The injections were performed using a Microinjector (ZGENEBIO, PCO-1500, Taipei, Taiwan). The SiNPs were injected at the ventral end of the Duct of Cuvier under a stereomicroscope (Nikon, SMZ645, Tokyo, Japan) and the pulse time was controlled to deliver 10 nL of SiNPs. After intravenous microinjection, zebrafish embryos were transferred to 6-well microplates (30 embryos in 3 mL solution/well) for a treatment period of 24 h. Zebrafish embryos injected with ultrapure water served as control group. For valid experiments, embryos were obtained only from spawns with a survival rate of the control group higher than 80%.

### Malformation assessment

After Albino zebrafish embryos injected with SiNPs (range from 1 to 12 mg/mL), the NOAEL was determined based on the modified morphological assessments as described before (Panzica-Kelly et al., 2010). Fifteen indicators of the morphological anatomic structures or organ systems (heart, circulation, edema, hemorrhage, head, jaw, eye, liver, intestine, somite, tail, notochord, muscle, fin, and swimming bladder) were abnormal defined as the zebrafish malformation. According to toxicology textbook and our preliminary experiments, 1/3 NOAEL, 2/3 NOAEL, NOAEL, 2 NOAEL, 4 NOAEL of SiNPs were chosen as the designed concentrations for the following experiments.

In addition, the pericardial edema, heart rate, and atria/ventricular ratio were detected as the cardiac toxicity phenotype induced by SiNPs.

### *o*-Dianisidine staining in cardiac section

After Albino zebrafish injected with SiNPs for 24 h, the embryos (72 hpf) were fixed by the 4% paraformaldehyde and overnight at 4 °C. Washing with PBST three times, the embryos were incubated in 0.6 mg/mL *o*-Dianisidine staining working solution (Sigma, USA) with 10 mM sodium acetate and 4% ethanol as previously described (Wu et al., 2011). Staining the embryos for 10 min in the dark at 28 °C and then washed three times with PBST. After that, the embryos with erythrocyte positive staining in cardiac section were observed under a stereomicroscope (Nikon, SMZ645, Tokyo, Japan). To analyze the relative numbers of erythrocyte, the Image-pro Plus software (Media Cybernetics, Bethesda, MD) was performed to calculate the average integrated optical density (IOD) for erythrocyte positive staining.

### Microarray analysis

For Affymetrix® microarray profiling, the total RNA was isolated from 30 zebrafish embryos per treatment group by the TRIzol reagent (Invitrogen, Carlsbad, Canada) and purified with an RNeasy Mini Kit (Qiagen, Hilden, Germany) according to the manufacturer's protocol. The amount and quality of RNA were determined by a UV-Vis Spectrophotometer (Thermo, NanoDrop 2000, USA) at the absorbance of 260 nm. The mRNA expression profiling was measured using Zebrafish Gene 1.0 ST Array (Affymetrix GeneChip®, Santa Clara, CA), which contains 59 302 gene-level probe sets. The microarray analysis was performed by Affymetrix® Expression Console Software (version 1.2.1, Santa Clara, CA). Raw data (CEL files) were normalized at transcript level using robust multi-array average method (RMA workflow). Median summarization of transcript expressions was calculated. Gene-level data was then filtered to include only those probe sets that are in the ''core'' metaprobe list, which represent RefSeq genes.

### Reactive oxygen species (ROS) assay

The whole-embryo ROS level was tested using an oxidation-sensitive probe, 5-(and 6-)-chloromethyl-2′,7′-dichloro-dihydro-fluorescein diacetate (CM-H2DCFDA, Life Technologies, Carlsbad, CA). Briefly, CM-H2DCFDA stock solution was diluted at a final concentration (0.5 μg/mL) for working solution. After exposed to SiNPs for 24 h, the embryos were incubated with 0.5 μg/mL CM-H2DCFDA for 1 h in dark at 28 °C. Then, rinsing three times with fish-husbandry water, the embryos were transferred into 96-well microplate (1 embryo per well) and the levels of whole-embryo ROS were tested with the absorbance at 488 nm under a multimode microplate reader (Berthold Technologies, LB940, Stuttgart, Germany).

### Inflammation detection by neutrophils-specific Tg(mpo:GFP) zebrafish

Neutrophils, in which cellular fluorescence is driven by the mpo (myeloperoxidase) promoter, were visualized in Tg(mpo:GFP) zebrafish injected with SiNPs at 2, 4, 24 hpi (hour post-injection), respectively. Then, the Tg(mpo:GFP) zebrafish embryos were examined immediately under a multi-purpose zoom fluorescence microscopy (Nikon, AZ100, Tokyo, Japan) at 2, 4, 24 hpi, respectively. The relative fluorescence was measured and quantified using Volocity Demo 6.1.1 software (PerkinElmer, Branford, CT).

### Histopathology

The zebrafish embryos samples were fixed in 10% formalin, embedded in paraffin, sectioned, and stained with hematoxylin and eosin for histological examination according to the standard techniques. After staining, the slides were observed and examined by optical microscope (Olympus X71-F22PH, Tokyo, Japan).

### Immunohistochemistry

After deparaffinization and rehydration, the paraffin-embedded samples were placed in a 10 mM citrate buffer solution and treated with 3% $H_2O_2$ in PBS for 5 min. Then, the samples were blocked with 10% normal goat serum for 10 min, and incubated overnight at 4 °C with primary antibody TNNT2 (ABCAM, London, UK) or an equivalent amount of normal goat IgG (CST, Boston, MA) as a negative control. After treated with avidin-biotin affinity system for 30 min at room temperature, and stained with 3-3′ diaminobenzidine substrate, the sections were examined under an optical microscope (Olympus X71-F22PH, Tokyo, Japan). All positive cells were carefully evaluated under double-blind conditions.

### Quantitative RT-PCR analysis

Total RNA was extracted from 50 zebrafish embryos per group using reagent (Invitrogen, Carlsbad, Canada) according to the manufacturer's protocol. Tissue incorporating all new tissue as well as one or two bone rays proximal to the original cut site was extracted. Equal amounts of total RNA from each sample were reverse transcribed with Thermoscript reverse transcriptase (Invitrogen) using oligo (dT) and random hexamer primers. qRT-PCR reaction was monitored by the ABI PRISM 7500 Sequence DetectionSystem (Applied Biosystems, Foster City, CA) and was run with three biological repeats and three duplicated repeats. All levels were normalized to β-actin (18S levels were similar) and fold induction was calculated by setting control conditions to 1. The primers are listed in Supplementary Table S1.

### Western blot analysis

Total protein of SiNPs-treated zebrafish was extracted with the Tissue Protein Rapid Extraction Kit (Keygen, China) and determined by performing the bicinchoninic acid (BCA) protein assay (Pierce, Waltham, MA). The equal amounts of 100 μg lysate proteins were loaded onto SDS-polyacrylamide gels (12%) and electrophoretically transferred to polyvinylidene difluoride membranes (Millipore, Billerica, MA). After blocking with 5% nonfat milk in TBST for 1 h at room temperature, the membrane was incubated with TNNT2 (1:1000, rabbit antibodies, Abcam, London, UK) overnight at 4 °C, After washed several times with TBST, the membrane was incubated with a horseradish peroxidase-conjugated anti-rabbit Ig G secondary antibody (Abcam, Britain) for 1 h at room temperature. Then, three times with TBST and the antibody-bound proteins were detected using the ECL chemiluminescence reagent (Pierce, Waltham, MA).

### Statistical analysis

All statistical analyses were performed using SPSS 16.0 software (SPSS, Chicago, IL). Student's *t*-test was performed for comparisons between two treatment groups. Three or more treatment groups were compared by one-way analysis of variance (ANOVA) followed by least significant difference (LSD) test. For bioinformatics analysis, differential expression genes were identified based on RVM *t*-test. Fisher's exact test was performed to select the significant pathway. Significance differences were considered at $p < 0.05$.

### Bioinformatics analysis

For microarray data analysis, differential expression genes were identified based on random variance model (RVM) *t*-test. And the differential expression genes were considered to be up or down regulated with at least $p < 0.05$. Genes with similar expression patterns often facilitate the overlapping functions. Accordingly, the cluster analysis of gene expression patterns was analyzed by Cluster and Java Treeview software. Pathway analysis was used to find out the significant pathway of the differential genes according to Kyoto Encyclopedia of Genes and Genomes (KEGG) database. Fisher's exact test was performed to select the significant pathway, and the threshold of significance was considered as $p < 0.05$.

## Results

### Characterization of SiNPs

The full characterization of SiNPs is presented in Figure 1. TEM images showed that the SiNPs exhibited a near-spherical shape and well dispersibility (Figure 1A). The size distribution showed that the average diameter of SiNPs was approximately $62.14 \pm 7.16$ nm (Figure 1B). The hydrodynamic sizes (Figure 1C) and zeta potentials (Figure 1D) of SiNPs in ultrapure water were approximately 106.8 nm and −38 mV, respectively. In addition, the purity of SiNPs was higher than 99.9% and no endotoxin was detected in SiNPs suspensions. Taken together, these results demonstrated that the SiNPs possessed favorable stability and monodispersity in microinjection medium.

### Cardiac toxicity phenotype

Based on the morphological assessments of zebrafish embryos, 3 mg/mL SiNPs was confirmed as the NOAEL of intravenous microinjection. A series of SiNPs concentrations (1, 2, 3, 6, 12 mg/mL) were then performed for the following cardiac toxicity experiments. Representative zebrafish malformation of cardiac region was shown in Figure 2A. Pericardial edema was the typical cardiac toxicity phenotype induced by SiNPs. The heart rate of zebrafish embryos was significantly decreased at the higher concentrations (6 and 12 mg/mL) compared to control group (Figure 2B). While the atria/ventricular ratio was 1:1 (Figure 2C), indicated that there was no atrioventricular block after zebrafish exposed to SiNPs.

### Erythrocyte detection

As shown in Figure 3, the relative numbers of erythrocyte in cardiac region were detected by hemoglobin staining with *o*-Dianisidine. At the lower concentration of SiNPs (3 mg/mL), the relative erythrocyte numbers was decreased significantly, which is 85.23% lower of control. These results demonstrated that the cardiac output was already declined even though there was no observed malformation in SiNPs-exposed zebrafish. It indicated that declined cardiac output induced by SiNPs could lead to cardiac dysfunction in zebrafish.

### Microarray analysis of zebrafish induced by SiNPs

From the hierarchical cluster analysis in Figure 4A, 2515 significant differential expression genes were obtained including 1107 genes were up-regulated and 1408 genes were down-regulated. The oxidative stress and inflammation-related genes were marked up-regulated. Based on KEGG database, the significant pathway analysis revealed that among 11 down-regulated genes significant pathways, calcium signaling pathway and cardiac muscle contraction were directly related to cardiac function (Figure 4B); while there was no up-regulated significant pathways associated to cardiac function. These two cardiac-related pathways, calcium signaling pathway and cardiac muscle

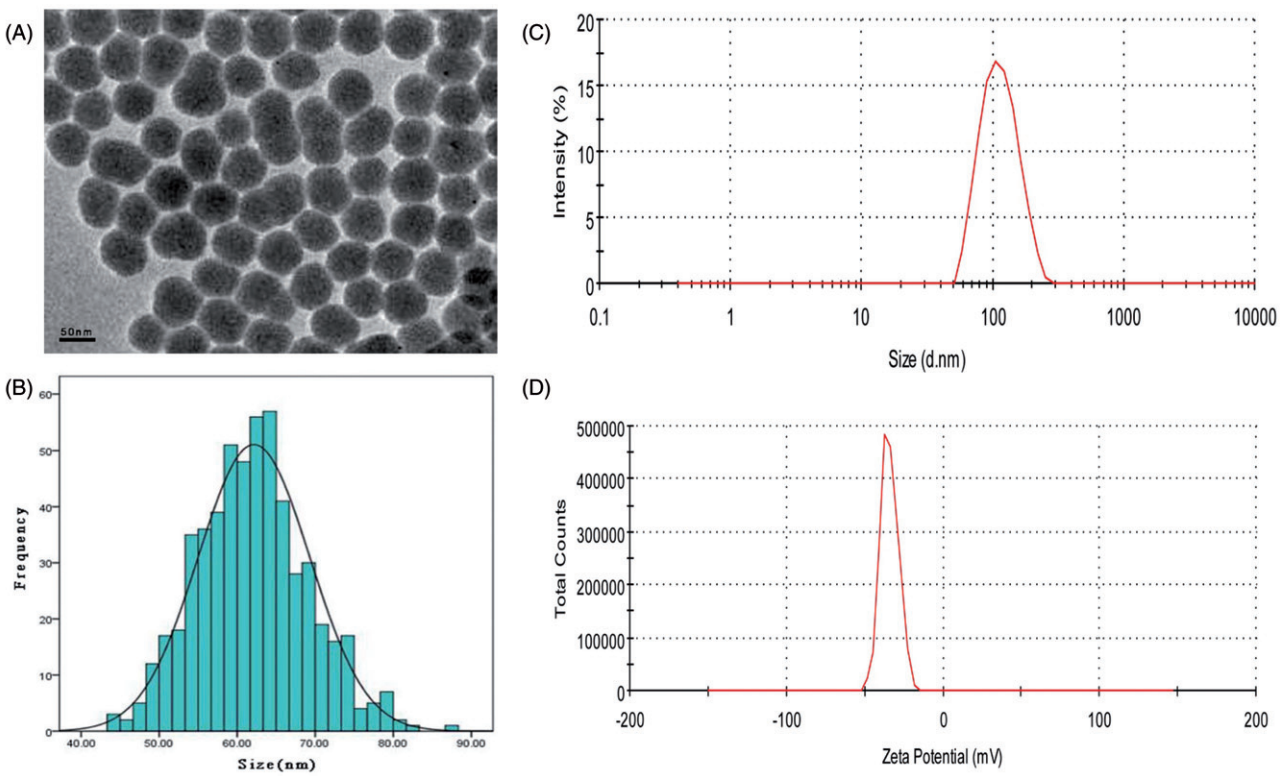


Figure 1. Characterization of SiNPs. (A) The SiNPs exhibited near-spherical shape with well dispersibility. Scale bar, 50 nm. (B) The average diameter of SiNPs was approximately $62.14 \pm 7.16$ nm. (C) The hydrodynamic sizes and (D) zeta potential of SiNPs in ultrapure water were approximately 106.8 nm and −38 mV, respectively.

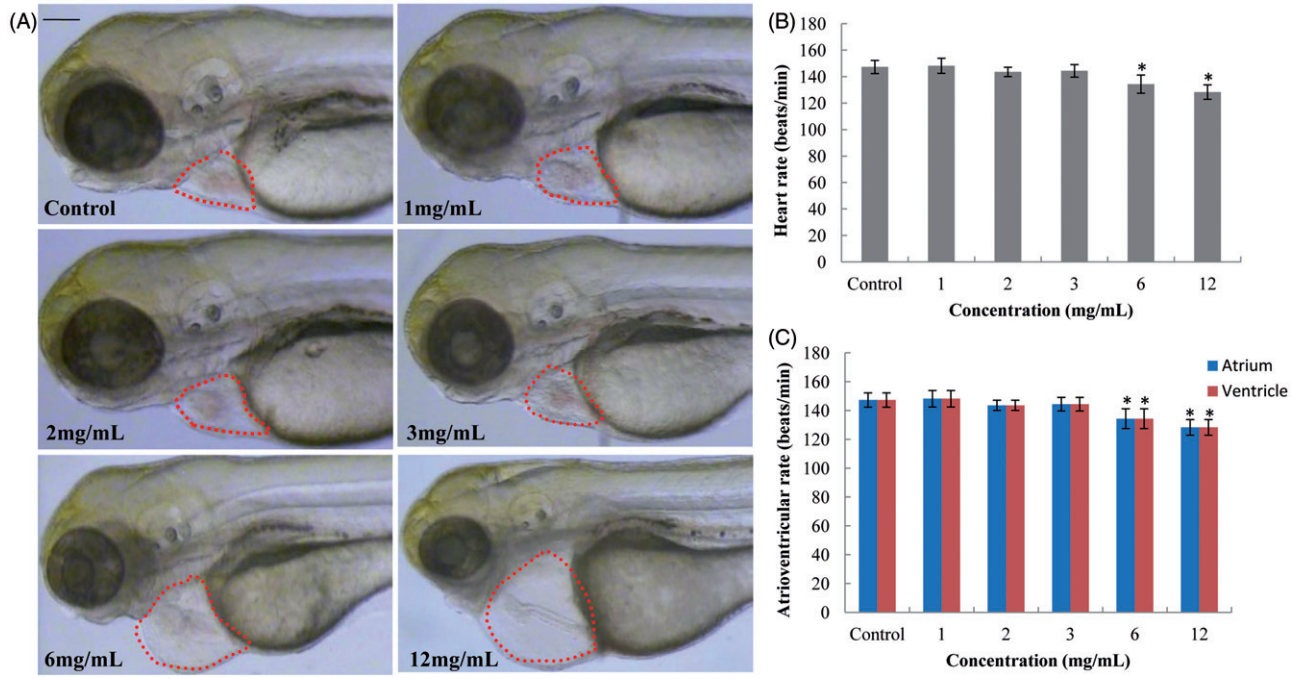


Figure 2. Cardiac toxicity phenotype induced by SiNPs. (A) Pericardial edema of zebrafish was the typical cardiac malformation. Scale bar: 100 μm. (B) Heart rate and (C) atrium and ventricle rate of zebrafish exposed to SiNPs at 72 hpf. Data are expressed as means ± S.D. from three independent experiments (*$p < 0.05$).

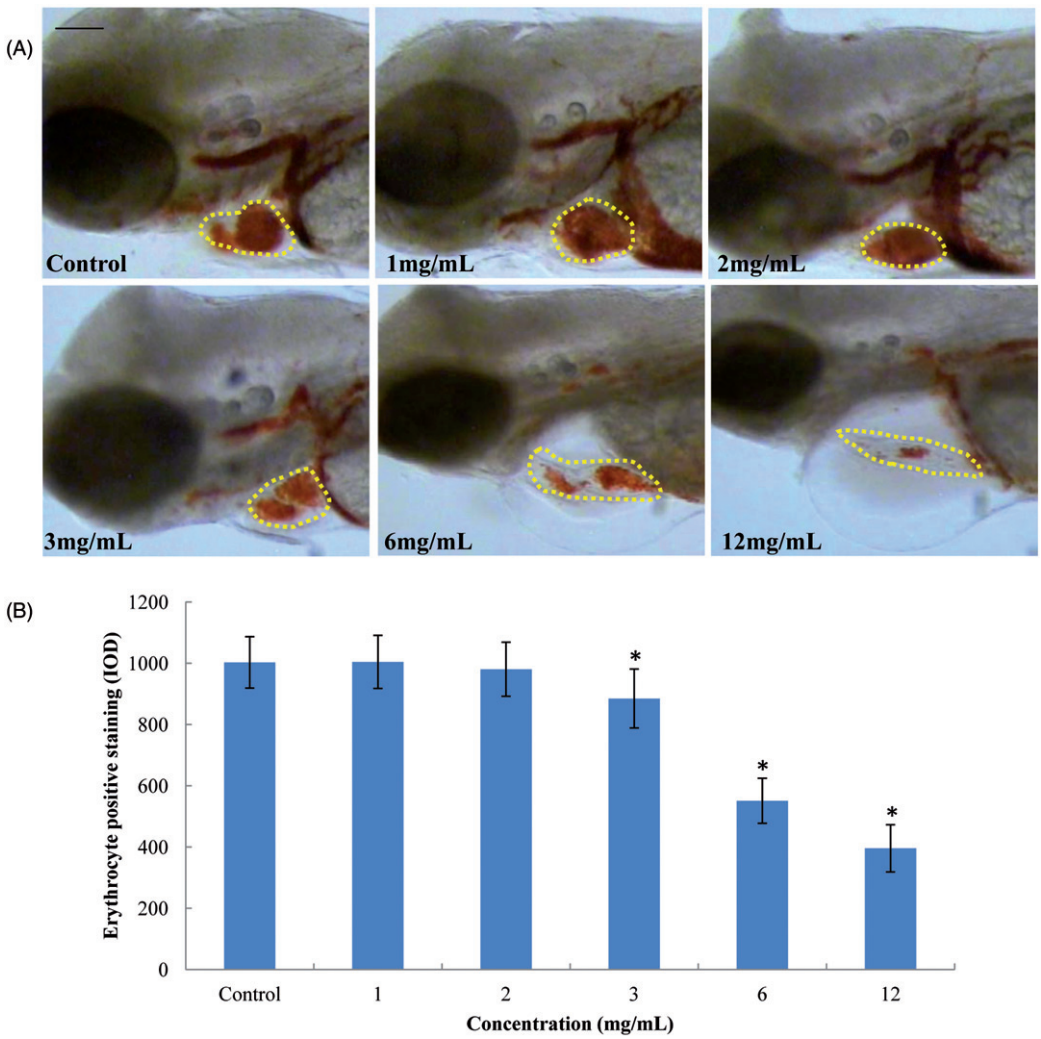


Figure 3. Erythrocyte detection in cardiac section of SiNPs-exposed zebrafish. (A) Erythrocyte was observed by *o*-Dianisidine staining. Scale bar: 100 μm. (B) The relative numbers of erythrocyte was performed by IOD analysis. Data are expressed as means ± S.D. from three independent experiments (*$p < 0.05$).

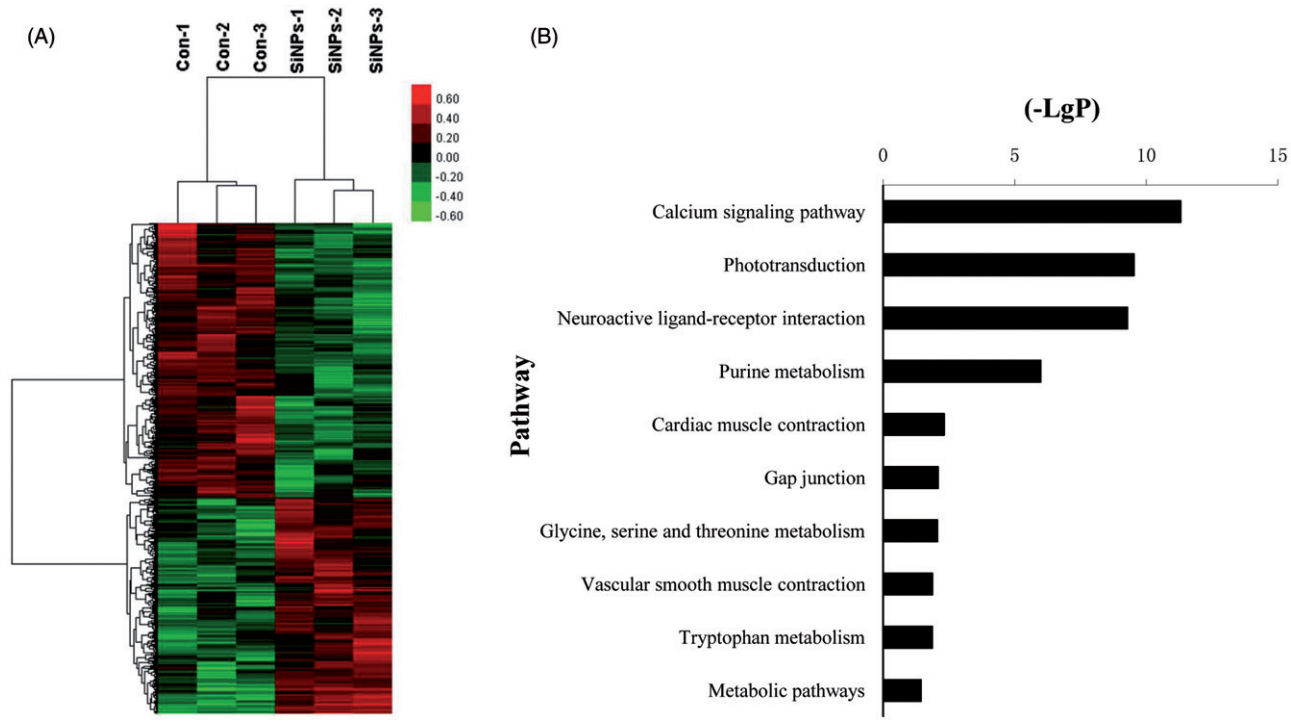


Figure 4. (A) Hierarchical cluster analysis of 2515 differential expression genes in zebrafish exposed to SiNPs. (B) Significant pathways of differential down-regulated expression genes based on KEGG database. –LgP, negative logarithm of the *p* value. X-axis denotes that the larger number with the smaller of *p* value.

contraction, contained 34 and 9 differential expression genes, respectively (Supplementary Table S2).

### Whole-embryo ROS measurement

To get a closer insight into the mechanisms of SiNPs on zebrafish embryos, we measured the ROS production via the fluorescence intensity of oxidation-sensitive probe (CM-H2DCFDA). As shown in Supplementary Figure S1, the whole-embryo ROS levels of all SiNPs-treated groups were increased gradually. At the highest concentration (12 mg/mL) of SiNPs, the fluorescence intensity was significantly elevated (2.6-fold as high as control). The results showed that SiNPs could induce the production of ROS in whole-embryo with a dose-dependent manner.

### Cardiac inflammation in Tg(mpo:GFP) zebrafish induced by SiNPs

Since the neutrophils are normally located in the ventral vein region, the recruitment and chemotaxis of neutrophils in Tg(mpo:GFP) zebrafish were observed mainly in the cardiac region after exposed to SiNPs (Figure 5A). The fluorescence intensity analysis demonstrated that the neutrophils were increased gradually at 2, 4, 24 hpi, respectively (Figure 5B). At the 2 hpi, only the higher concentrations of SiNPs (6 and 12 mg/mL) had significant difference compared to control group. As the time increasing, the intensity of neutrophils in NOAEL level of SiNPs (3 mg/mL) was elevated significantly in 4 hpi. At 24 hpi, all the treatment groups except 2 mg/mL of SiNPs were significantly increased compared to that of control. The results indicated that SiNPs induced cardiac inflammation in a dose- and time-dependent way in zebrafish embryos.

### Histopathological examination and immunohistochemistry analysis

As shown in Figure 6A and 6B, there was no marked morphological change of ventricle and atrium in control group or in SiNPs-treated group by histopathological examination. Both endothelial cells and cardiomyocytes had normal cell shape in SiNPs-treated group. However, few inflammatory cells were observed in atrium of SiNPs-treated zebrafish heart (Figure 6B). The cardiac contraction marker protein TNNT2 was measured in heart tissue of zebrafish embryos using immunohistochemistry. The staining of TNNT2 positive cells in the treatment group (Figure 6C) had a much weaker expression than that in the control group (Figure 6D). Taken together, it indicated that SiNPs might trigger the inflammatory response and inhibit the cardiac contraction in zebarfish embryos even at very low dosage.

### Effect of SiNPs on calcium signaling pathway and cardiac muscle contraction

The expression of genes in calcium signaling pathway and cardiac muscle contraction of zebrafish embryos were examined according to gene chip high-throughput screening and significant pathway analysis (Figure 7A). qRT-PCR analysis showed that the genes regulated to ATPase (*atp2a1l*, *atp1b2b*, *atp1a3b*), calcium channel (*cacna1ab*, *cacna1da*), cardiac troponin C (*tnnc1a*) were down-regulated (Figure 7B). In addition, the expression of cardiac contraction marker TNNT2 protein was decreased in a dose-dependent manner after zebrafish exposed to SiNPs (Figure 7C and D). A schematic model of the molecular mechanisms on low-dose exposure of SiNPs-induced cardiac dysfunction in zebrafish embryos was presented in Figure 8.

## Discussion

In our daily life, the exposure of nanoparticles to human being is often at very low concentrations, but exposed day-to-day. This study was aimed to evaluate the cardiac toxicity mechanism of SiNPs in zebrafish at low-dose exposure. Although the pericardial edema is one of the common abnormal phenotypes in zebrafish induced by nanomaterials (Kim et al., 2014; Park et al., 2013), the underlying mechanism is still unknown. For the first time, we

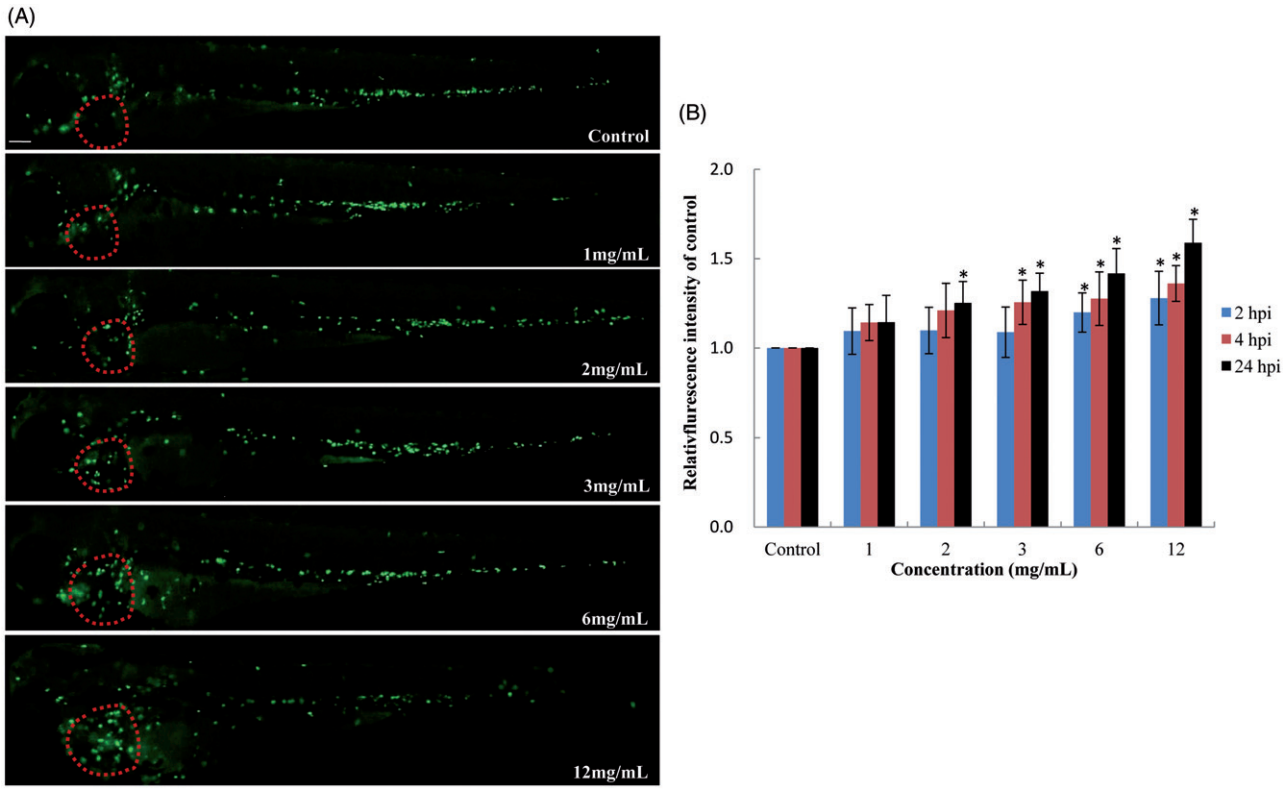


Figure 5. Cardiac inflammation in Tg(mpo:GFP) zebrafish induced by SiNPs. (A) Neutrophils were recruited and migrated in cardiac region. Scale bar: 100 μm. (B) The relative fluorescence intensity of neutrophils were increased markedly at 2, 4, 24 hpi, respectively. Data are expressed as means ± S.D. from three independent experiments (*$p < 0.05$).

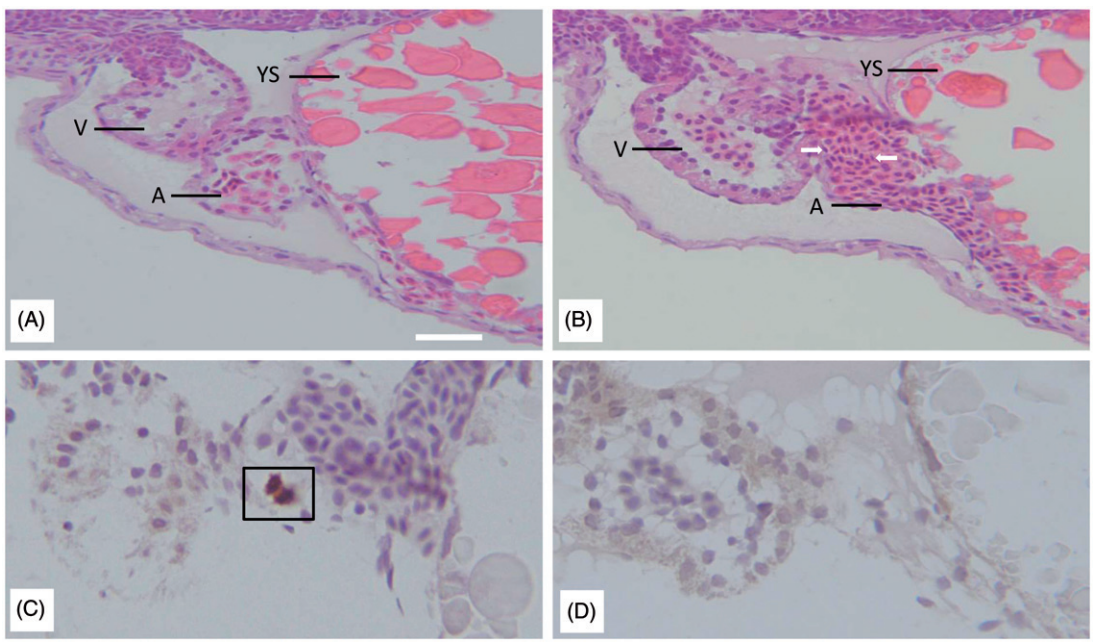


Figure 6. Histopathological examination and immunohistochemistry analysis of zebrafish heart induced by SiNPs. A and C: Control group; B and D, SiNPs-treated group. (A and B) SiNPs-treated zebrafish showed few inflammatory cells in heart tissue. V, ventricle; A, atrium; YS, yolk sac. White arrows indicate inflammatory cells. (C and D) The cardiac contraction marker TNNT2 protein had a much weaker expression than control group in heart tissue using immunohistochemistry. Black box denotes the positive cells. Scale bar: 20 μm.

demonstrated that SiNPs induced cardiac dysfunction via neutrophil-mediated inflammation and cardiac muscle contraction in zebrafish embryos.

Consistent with our previous study (Duan et al., 2013b), either from water-born exposure or intravenous microinjection, SiNPs could induce pericardial edema and inhibited the heart rate in zebrafish embryos (Figure 2A and B), which resulted in bradycardia. We further measured the atria and ventricular rate to analyze whether SiNPs triggered the atrioventricular block in zebrafish embryos. The atria/ventricular ratio was 1:1 from control group or SiNPs-treated groups (Figure 2C). Abnormal heart rhythm observed in zebrafish usually contains tachycardia,

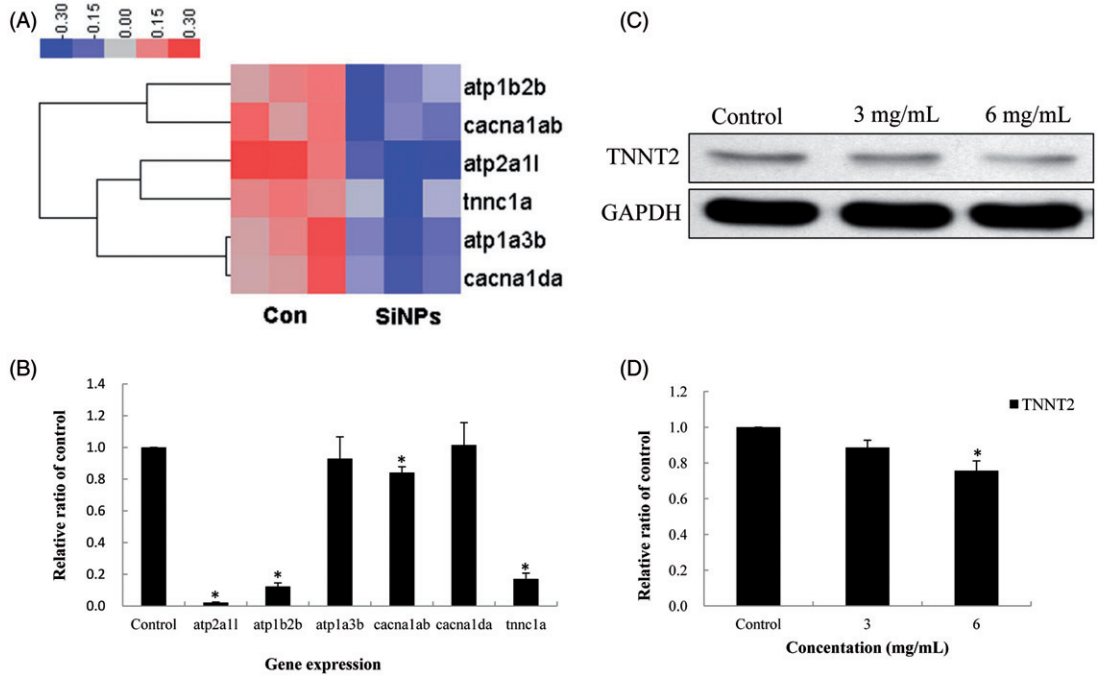


Figure 7. Effect of SiNPs on calcium signaling pathway and cardiac muscle contraction. (A) Heat map from microarray analysis of genes expression related to significant pathway. (B) qRT-PCR analysis showed that the genes involved in calcium signaling pathway and cardiac muscle contraction were decreased. (C) Effect of SiNPs on cardiac-specific protein TNNT2. (D) Relative densitometric analysis showed that the expression of TNNT2 was down-regulated induced by SiNPs. Data are expressed as means ± S.D. from three independent experiments (*$p < 0.05$).

bradycardia, atrioventricular block, and premature contraction or fibrillation (Zhu et al., 2014). These results indicated SiNPs had a toxic effect on heart rhythm, especially on bradycardia; but had no effect on atrioventricular block. The results demonstrated that low-dose exposure of SiNPs indeed triggered cardiac toxicity in zebrafish embryos, and the change of heart rhythm may have a bad influence on cardiac function.

Since cardiac output is a sensitive indicator for cardiac function, we performed erythrocyte staining with *o*-Dianisidine to reflect the cardiac output in living zebrafish embryos (Figure 3). Our results suggested that the cardiac output was already changed even though there was no observed malformation in SiNPs-exposed embryos. The changes in cardiac output are as a result of cardiac contraction disturbances (Choi & Park, 2012). Up to now, few studies are focused on the relationship between cardiac output and nanoparticles exposure. In line with our findings, Szebeni and coworkers found that liposomes and lipid-based nanoparticles could cause cardiac arrhythmias and decline the cardiac output in pig model (Szebeni et al., 2007). While other study reported that the gel formation of core/shell nanoparticles improved the cardiac functions, especially on the cardiac output and ejection fraction (Oh et al., 2010). The controversial conclusions required more studies to explore the toxic mechanisms of nanoparticles on cardiac function. In generally, the decreasing of cardiac output will lead to increase of heart rate in physiologic compensatory reaction of organism. However, either from our previous study with water-born exposure or this study with intravenous microinjection, we found the heart rate was declined in a dose-dependent manner rather than elevating in SiNPs-treated zebrafish. Our results indicated the changing trend of heart rate was in step with cardiac output (Figures 2B and 3). Why we didn't observe the physiologic compensatory reaction in zebrafish? Perhaps the main cause of this phenomenon is due to one of the distinct advantages in zebrafish: the embryos can survive for several days via the passive transport of oxygen without cardiovascular circulation (Liu & Stainier, 2012). So the zebrafish embryos did not need to accelerate the heart rate for oxygen intake to response the lower cardiac output induced by SiNPs.

To get a deep insight into the mechanisms of SiNPs on cardiac function in zebrafish, we performed the microarray analysis and bioinformatics analysis to screen the significant differential expression genes and possible pathways (Figure 4). Our data found that the oxidative stress and inflammation related genes were marked up-regulated. It is well known that the oxidative stress and inflammation are two major mechanisms for nanoparticles-caused toxicity *in vivo* or *in vitro* (Alinovi et al., 2015; Khatri et al., 2013; Mendoza et al., 2014). The surface chemical structure of SiNPs contain a lot of hydroxyl radical (·OH), which has a great tendency to induce oxidative stress and cause extensive damage in cells (Duan et al., 2013a). Our results showed that SiNPs increased the level of ROS in whole-embryo with a dose-dependent way (Figure S1). Using Tg(mpo:GFP) zebrafish, the recruitment and chemotaxis of neutrophils induced by SiNPs were observed in cardiac region (Figure 5). The accumulation of neutrophils leads to produce an inflammatory response and exacerbate the myocardial injury (Saeed et al., 2005). It was reported that SD rats exposed to ZnO nanoparticles via intratracheal instillation increased the levels of neutrophils, lactate dehydrogenase, and total protein in bronchoalveolar lavage fluid (Chuang et al., 2014). Yet, there was no report on the toxicity of nanoparticles-induced neutrophils accumulation and cardiac inflammation in living organism. MPO, an abundant lysosomal enzyme, is presented in the granules of mature human neutrophils and eosinophils. In zebrafish, the MPO was only positive expressed in neutrophil granules, so the positive expression of MPO is a specific marker for neutrophil and can reflect the neutrophil distribution and inflammatory response in zebrafish (Bennett et al., 2001). The neutrophils are normally located in the ventral vein region and distributed throughout the embryo via circulation. To inflammatory response, the neutrophil recruitment is driven by departure from the ventral vein region and migrated

to the injured tissue (Shen et al., 2013). In this study, we used Tg(mpo:GFP) transgenic zebrafish line to visualize the inflammatory response induced by SiNPs. For the first time, our results found that the cardiac inflammation was strongly linked with the SiNPs exposure in zebrafish by *in vivo* observation. And we also observed few inflammatory cells were existed in SiNPs-treated zebrafish heart by histopathological examination (Figure 6A and B). In addition, the cardiac-specific protein TNNT2 was expressed much weaker than control group in heart tissue of embryos using immunohistochemistry (Figure 6C and D). Taken together, it indicated that the cardiac inflammation induced by SiNPs might lead to cardiac injury in zebrafish embryos.

Based on KEGG database, the significant pathway analysis revealed that calcium signaling pathway and cardiac muscle contraction were directly related to cardiac function in zebrafish embryos (Figure 4B). Then, the validity experiments were performed by qRT-PCR and western blot assays. As shown in Figure 7A and B, the SiNPs inhibited the calcium signaling pathway and cardiac muscle contraction via the down-regulation of *atp2a1l*, *atp1b2b*, *atp1a3b*, *cacna1ab*, *cacna1da*, and *tnnc1a*. The *atp2a1l*, *atp1b2b*, *atp1a3b* are regulated to the ATPase and $Ca^{2+}$ transporting; the *cacna1ab*, *cacna1da* are controlling genes for voltage-dependent calcium channel; while the *tnnc1a* is a regulatory gene for cardiac troponin C. Cardiac muscle contraction is a complex process involved in cardiomyocyte stimulation and membrane depolarization, increased of intracellular $Ca^{2+}$ level and ATPase activity, going with the production of cardiac muscle dynamics (Katrukha, 2013). The key role in the regulation of muscle contraction is the structure changes in troponin complex (Marx & Marks, 2013). In this study, our findings demonstrated that SiNPs could reduce the cardiac muscle contraction via the down-regulation of related genes in ATPase, calcium channel, and cardiac troponin C.

Besides the gene-level detection, the cardiac-specific protein TNNT2 was also measured to verify the inhibition of cardiac muscle contraction induced by SiNPs. The protein level of TNNT2 was decreased in a dose-dependent manner (Figure 7C and D). Knockdown of *tnnt2* in zebrafish embryos had been proved to specifically block cardiac muscle contractility and lead to cardiotoxicity (Chen, 2013). In addition, some studies reported that TNNT2 was also required for sarcomeres formation and function. In *tnnt2* mutation zebrafish, the loss of sarcomere and disarray of myocyte were observed with reduction of thin filament gene expression (Sehnert et al., 2002). Disruption of sarcomeres and failure of cardiac contraction lead to die in during embryogenesis in *tnnt2*$^{-/-}$ mice (Nishii et al., 2008). The reduction of cardiac muscle contraction is an important hallmark of severe heart diseases, such as cardiomyopathy and heart failure (Marks, 2013). Among these diseases, the cardiac muscle contraction is insufficient to supply enough blood required by other organs. This syndrome is a common complication ensuing from a serious of cardiovascular pathologies. Based on the results mentioned above, a schematic representation of the mechanisms on cardiac dysfunction induced by low-dose exposure of SiNPs was presented in Figure 8.

Up to now, only a few studies focused on the cardiac muscle contraction induced by nanoparticles. It was reported that the decreasing myocardial contractility occurred due to the toxicity with high dose of silver nanoparticles in Ross broiler chickens (Raieszadeh et al., 2013). While in our study, we found that the decreased of cardiac muscle contraction occurred even in low-dose exposure of SiNPs Our data provide new evidence on the cardiac toxicity after vertebrate exposure to nanoparticles at lower concentrations. It will in turn be helpful in managing risk and providing guidance for reducing hazardous effect of nano-scale particles.

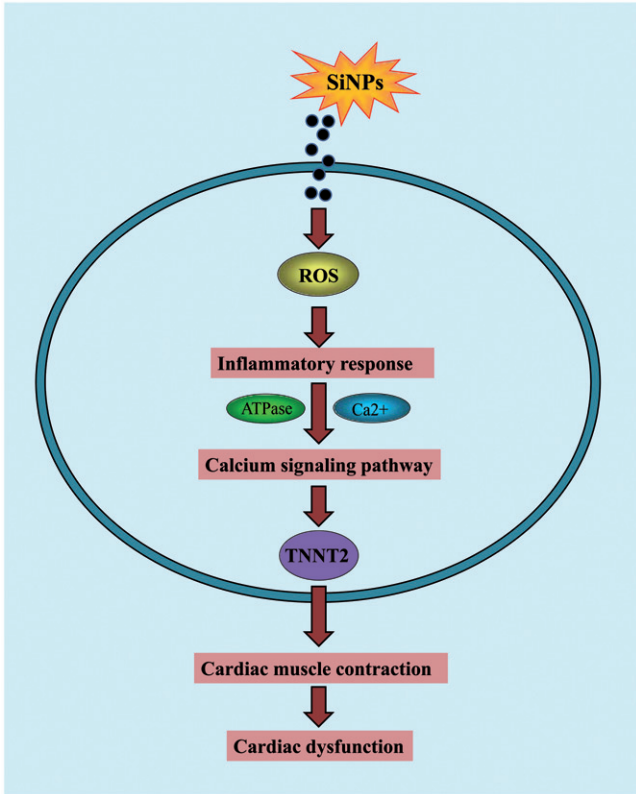


Figure 8. Schematic representation of cardiac dysfunction induced by low-dose SiNPs.

## Conclusions

In this study, using intravenous microinjection we explored the cardiac dysfunction induced by low-dose exposure of SiNPs in zebrafish and found that: SiNPs induced cardiac toxicity phenotypes including the pericardial edema and bradycardia, but had no effect on atrioventricular block. The decreased of cardiac output in zebrafish embryos was triggered by oxidative stress and neutrophil-mediated cardiac inflammation. In addition, SiNPs inhibited the calcium signaling pathway and cardiac muscle contraction pathway via the down-regulation-related genes of ATPase, calcium channel, and cardiac troponin C and decreased the protein level of cardiac contraction marker protein TNNT2. Our study clarified for the first time that low-dose exposure of SiNPs induced cardiac dysfunction via neutrophil-mediated cardiac inflammation and cardiac contraction in zebrafish embryos. The present study also highlights the importance of cardiotoxicity evaluation of nanomaterials at low-level exposure.

## Acknowledgements

The authors thank Prof. Wensheng Yang from Jilin University for the preparation of SiNPs, and Weiping Tang of Genminix Informatics for bioinformatics assistance.

## Declaration of interest

The authors declare they have no conflict of interest. This work was supported by National Natural Science Foundation of China (no. 81230065), Special Project of Beijing Municipal Science & Technology Commission (KZ201410025022), and Training Programme Foundation for the Talents by the Beijing Ministry of Education (2014000020124G152).

## References


Alinovi R, Goldoni M, Pinelli S, Campanini M, Aliatis I, Bersani D, et al. 2015. Oxidative and pro-inflammatory effects of cobalt and titanium oxide nanoparticles on aortic and venous endothelial cells. Toxicol In Vitro 29:426–37.

Bakkers J. 2011. Zebrafish as a model to study cardiac development and human cardiac disease. Cardiovasc Res 91:279–88.

Bauer AT, Strozyk EA, Gorzelanny C, Westerhausen C, Desch A, Schneider MF, Schneider SW. 2011. Cytotoxicity of silica nanoparticles through exocytosis of von Willebrand factor and necrotic cell death in primary human endothelial cells. Biomaterials 32:8385–93.

Becker JR, Deo RC, Werdich AA, Panakova D, Coy S, Macrae CA. 2011. Human cardiomyopathy mutations induce myocyte hyperplasia and activate hypertrophic pathways during cardiogenesis in zebrafish. Dis Model Mech 4:400–10.

Benard EL, van der Sar AM, Ellett F, Lieschke GJ, Spaink HP, Meijer AH. 2012. Infection of zebrafish embryos with intracellular bacterial pathogens. J Vis Exp 15:pii:3781.

Benezra M, Penate-Medina O, Zanzonico PB, Schaer D, Ow H, Burns A, et al. 2011. Multimodal silica nanoparticles are effective cancer-targeted probes in a model of human melanoma. J Clin Invest 121: 2768–80.

Bennett CM, Kanki JP, Rhodes J, Liu TX, Paw BH, Kieran MW, et al. 2001. Myelopoiesis in the zebrafish, Danio rerio. Blood 98:643–51.

Brook RD, Rajagopalan S, Pope 3RD CA,, Brook JR, Bhatnagar A, Diez-Roux AV, et al. 2010. Particulate matter air pollution and cardiovascular disease: an update to the scientific statement from the American Heart Association. Circulation 121:2331–78.

Chen J. 2013. Impaired cardiovascular function caused by different stressors elicits a common pathological and transcriptional response in zebrafish embryos. Zebrafish 10:389–400.

Choi SW, Park SM. 2012. Analysis of left ventricular impedance in comparison with ultrasound images. Artif Organs 36:479–86.

Chuang HC, Juan HT, Chang CN, Yan YH, Yuan TH, Wang JS, et al. 2014. Cardiopulmonary toxicity of pulmonary exposure to occupationally relevant zinc oxide nanoparticles. Nanotoxicology 8:593–604.

Du Z, Zhao D, Jing L, Cui G, Jin M, Li Y, et al. 2013. Cardiovascular toxicity of different sizes amorphous silica nanoparticles in rats after intratracheal instillation. Cardiovasc Toxicol 13:194–207.

Duan J, Yu Y, Li Y, Yu Y, Li Y, Zhou X, et al. 2013a. Toxic effect of silica nanoparticles on endothelial cells through DNA damage response via Chk1-dependent G2/M checkpoint. PLoS One 8:e62087.

Duan J, Yu Y, Li Y, Yu Y, Sun Z. 2013b. Cardiovascular toxicity evaluation of silica nanoparticles in endothelial cells and zebrafish model. Biomaterials 34:5853–62.

Duan J, Yu Y, Yu Y, Li Y, Huang P, Zhou X, et al. 2014a. Silica nanoparticles enhance autophagic activity, disturb endothelial cell homeostasis and impair angiogenesis. Part Fibre Toxicol 11:50.

Duan J, Yu Y, Yu Y, Li Y, Wang J, Geng W, et al. 2014b. Silica nanoparticles induce autophagy and endothelial dysfunction via the PI3K/Akt/mTOR signaling pathway. Int J Nanomedicine 9: 5131–41.

Ferrante MI, Kiff RM, Goulding DA, Stemple DL. 2011. Troponin T is essential for sarcomere assembly in zebrafish skeletal muscle. J Cell Sci 124:565–77.

Gold DR, Mittleman MA. 2013. New insights into pollution and the cardiovascular system: 2010 to 2012. Circulation 127:1903–13.

Hansen SF, Michelson ES, Kamper A, Borling P, Stuer-Lauridsen F, Baun A. 2008. Categorization framework to aid exposure assessment of nanomaterials in consumer products. Ecotoxicology 17:438–47.

Katrukha IA. 2013. Human cardiac troponin complex. Structure and functions. Biochemistry (Mosc) 78:1447–65.

Keller AA, Mcferran S, Lazareva A, Suh S. 2013. Global life cycle releases of engineered nanomaterials. J Nanopart Res 15:1–17.

Khatri M, Bello D, Gaines P, Martin J, Pal AK, Gore R, Woskie S. 2013. Nanoparticles from photocopiers induce oxidative stress and upper respiratory tract inflammation in healthy volunteers. Nanotoxicology 7: 1014–27.

Kim MS, Louis KM, Pedersen JA, Hamers RJ, Peterson RE, Heideman W. 2014. Using citrate-functionalized $TiO_2$ nanoparticles to study the effect of particle size on zebrafish embryo toxicity. Analyst 139: 964–72.

Kumar P, Robins A. 2010. A review of the characteristics of nanoparticles in the urban atmosphere and the prospects for developing regulatory controls. Atmos Environ 44:5035–52.

Lee KJ, Browning LM, Nallathamby PD, Desai T, Cherukuri PK, Xu XH. 2012. In vivo quantitative study of sized-dependent transport and toxicity of single silver nanoparticles using zebrafish embryos. Chem Res Toxicol 25:1029–46.

Liu J, Stainier DY. 2012. Zebrafish in the study of early cardiac development. Circ Res 110:870–4.

Liu X, Sun J. 2010. Endothelial cells dysfunction induced by silica nanoparticles through oxidative stress via JNK/P53 and NF-kappaB pathways. Biomaterials 31:8198–209.

Marks AR. 2013. Calcium cycling proteins and heart failure: mechanisms and therapeutics. J Clin Invest 123:46–52.

Marx SO, Marks AR. 2013. Dysfunctional ryanodine receptors in the heart: new insights into complex cardiovascular diseases. J Mol Cell Cardiol 58:225–31.

Mathias JR, Dodd ME, Walters KB, Yoo SK, Ranheim EA, Huttenlocher A. 2009. Characterization of zebrafish larval inflammatory macrophages. Dev Comp Immunol 33:1212–17.

Mendoza A, Torres-Hernandez JA, Ault JG, Pedersen-Lane JH, Gao D, Lawrence DA. 2014. Silica nanoparticles induce oxidative stress and inflammation of human peripheral blood mononuclear cells. Cell Stress Chaperones 19:777–90.

Nishii K, Morimoto S, Minakami R, Miyano Y, Hashizume K, Ohta M, et al. 2008. Targeted disruption of the cardiac troponin T gene causes sarcomere disassembly and defects in heartbeat within the early mouse embryo. Dev Biol 322:65–73.

OECD. 2010. O. F. E. C.-O. A. D. Series on the safety of manufactured nanomaterials No. 27-ENV/JM/MONO(2010)46. Available at: http://www.oecd.org/science/nanosafety/.

Oh KS, Song JY, Yoon SJ, Park Y, Kim D, Yuk SH. 2010. Temperature-induced gel formation of core/shell nanoparticles for the regeneration of ischemic heart. J Control Release 146:207–11.

Panzica-Kelly JM, Zhang CX, Danberry TL, Flood A, Delan JW, Brannen KC, Augustine-Rauch KA. 2010. Morphological score assignment guidelines for the dechorionated zebrafish teratogenicity assay. Birth Defects Res B Dev Reprod Toxicol 89:382–95.

Park K, Tuttle G, Sinche F, Harper SL. 2013. Stability of citrate-capped silver nanoparticles in exposure media and their effects on the development of embryonic zebrafish (*Danio rerio*). Arch Pharm Res 36:125–33.

Pope 3rd CA, Burnett RT, Thurston GD, Thun MJ, Calle EE, Krewski D, Godleski JJ. 2004. Cardiovascular mortality and long-term exposure to particulate air pollution: epidemiological evidence of general pathophysiological pathways of disease. Circulation 109:71–7.

Raieszadeh H, Noaman V, Yadegari M. 2013. Echocardiographic assessment of cardiac structural and functional indices in broiler chickens treated with silver nanoparticles. ScientificWorldJournal 2013:931432.

Saeed SA, Waqar MA, Zubairi AJ, Bhurgri H, Khan A, Gowani SA, et al. 2005. Myocardial ischaemia and reperfusion injury: reactive oxygen species and the role of neutrophil. J Coll Physicians Surg Pak 15: 507–14.

Sehnert AJ, Huq A, Weinstein BM, Walker C, Fishman M, Stainier DY. 2002. Cardiac troponin T is essential in sarcomere assembly and cardiac contractility. Nat Genet 31:106–10.

Shen LJ, Cao LF, Chen FY, Zhang Y, Zhong JH, Zhong H. 2013. Using modified whole-mount in situ hybridization to study mpo expression in zebrafish. Exp Ther Med 5:1043–7.

Sogah VM, Serluca FC, Fishman MC, Yelon DL, Macrae CA, Mably JD. 2010. Distinct troponin C isoform requirements in cardiac and skeletal muscle. Dev Dyn 239:3115–23.

Szebeni J, Alving CR, Rosivall L, Bunger R, Baranyi L, Bedocs P, et al. 2007. Animal models of complement-mediated hypersensitivity reactions to liposomes and other lipid-based nanoparticles. J Liposome Res 17:107–17.

Tsetskhladze ZR, Canfield VA, Ang KC, Wentzel SM, Reid KP, Berg AS, et al. 2012. Functional assessment of human coding mutations affecting skin pigmentation using zebrafish. PLoS One 7:e47398.

World Health Organization. 2014. World Health Statistics. Available at: http://www.who.int/gho/publications/world_health_statistics/en/.

Wu YT, Lin CY, Tsai MY, Chen YH, Lu YF, Huang CJ, et al. 2011. beta-Lapachone induces heart morphogenetic and functional defects by promoting the death of erythrocytes and the endocardium in zebrafish embryos. J Biomed Sci 18:70.

Xu Z, Zhang YL, Song C, Wu LL, Gao HW. 2012. Interactions of hydroxyapatite with proteins and its toxicological effect to zebrafish embryos development. PLoS One 7:e32818.

Yu Y, Li Y, Wang W, Jin M, Du Z, Li Y, et al. 2013. Acute toxicity of amorphous silica nanoparticles in intravenously exposed ICR mice. PLoS One 8:e61346.

Zhu JJ, Xu YQ, He JH, Yu HP, Huang CJ, Gao JM, et al. 2014. Human cardiotoxic drugs delivered by soaking and microinjection induce cardiovascular toxicity in zebrafish. J Appl Toxicol 34: 139–48.

**Supplementary material available online**

Supplementary Figure S1 and Tables S1 - S2